23rd International Conference on Renewable Energies and Power Quality (ICREPQ'25)
Tenerife (Spain), 25th to 27th June 20245
Renewable Energy and Power Quality Journal (RE&PQJ)
ISSN 2172-038 X, Volume No.23, September 2025

Three-phase four-wire Buck-Boost Modular Converter with Active Power Filter Functionality

F. Barrero-González, M.I. Milanés-Montero, Eva González-Romera, C. Roncero-Clemente, J. Gutiérrez-Escalona, and E. Romero-Cadaval

[1] Department of Electrical, Electronic and Automatic Engineering
Escuela de Ingenierías Industriales, Universidad de Extremadura
Av. Elvas sn. 06006 Badajoz (Spain)

Abstract. This study enhances the buck-boost modular converter topology, also known as the Y-voltage source inverter, by implementing a control strategy that simultaneously manages active power injection into the grid while functioning as a shunt active power filter. Each phase-module operates as an independent buck-boost dc-dc converter, allowing the converter to accommodate wide variations in photovoltaic (PV) voltage. The control strategy is derived from instantaneous id-iq power theory and employs a dead-beat-type current control, which is developed and validated. Simulation tests confirm the converter's efficiency as an Active Power Filter (APF) under unbalanced and distorted grid voltage conditions.

Key words. Four-wire converters, Hybrid microgrid, Three-phase dc–ac converter, Universal converter, Active power filter.

1. Introduction

The integration of dc and ac distribution networks is an emerging reality. Dual-purpose Power Converters (PCs) [1] have been developed as transitional technologies to support the integration of Renewable Energy Sources (RESs) and Energy Storage Systems (ESS) into diverse grid configurations, prioritizing performance and versatility. These dc-dc/ac converters employ the same terminals, semiconductors, and passive components for both conversion modes, minimizing additional components. Given the diverse nature of Distributed Energy Resources (DERs), bidirectional buck and boost capabilities over a broad voltage range are essential. Furthermore, modular power converter structures enhance flexibility across multiple power conversion applications.

Several topologies have been previously proposed, along with their design and sizing, as well as some modulation techniques [2]-[4]. Paper [2] introduced a new member to the universal converter family, which is suitable for dc and three-phase ac applications. Each phase-module functions independently as a buck-boost dc-dc converter, offering a simple operational approach. Thereby, it effectively copes with a wide variation of the dc input source.

When required to operate as an inverter connected to a three-phase four-wire network, three of the branches or cells synthesize a dc-biased sinusoidal voltage wave because only unipolar voltage is feasible. with each phase displaced by $2\pi/3$ radians; the fourth branch, acting as source neutral-wire, has to synthesize the necessary offset dc voltage. On the other hand, during the dc–dc power conversion, the buck-boost branches are paralleled.

A similar concept was presented in [5], denoted in that paper as Y-voltage source inverter (VSI), and used for three-phase three-wire variable speed ac drives. Reference [6] introduces a three-phase four-wire topology that serves as an interlinking converter for hybrid ac/dc microgrids, where the ac microgrid neutral is directly connected to the positive terminal of the dc microgrid.

However, the application to the case of integrating dc sources, including PV, into the grid, simultaneously considering their interaction and exploiting the possibility of providing ancillary services, has not yet been addressed in detail. And then, moving a step further, this paper this paper addresses this gap by implementing a control strategy that regulates active power injected into the grid (extracting the maximum or a reference power from PV panels), functioning as a shunt APF simultaneously, injecting or demanding reactive power and compensating unbalanced and harmonic current components from non-linear loads connected at the Point of Common Coupling (PCC). The two functionalities must show a successful performance under distorted and unbalanced grid voltage. To accomplish this, a set of inverter output reference currents is generated by the control strategy based on the instantaneous id -iq power theory.

Concerning the current controller, in the dead-beat implementation originally presented in [7], a discrete-time model is used to predict the current trajectory one or more sampling periods in advance, to determine the plant input (i.e., the duty cycle) that makes the reference tracking error equal to zero at the same number of periods. The controller

is characterized by a relatively low complexity and, at the same time, by a very good dynamic performance. It is regarded as one of the best choices for obtaining a good tracking of the reference currents at converter output [8]-[11]. Nevertheless, its application to the dc-dc/ac buck-boost modular converter adding APF functionality has not been proved. This study develops and validates an improved dead-beat controller tailored to this topology.

Summarizing, the main contribution of this paper are as follows:

1. The proposal of a three-phase four-wire member of the universal converter family, being suitable for dc and three-phase ac, adding, for the first time, the implementation of a control strategy, which simultaneously controls the active power injected into the grid (RPP and MPPT modes) and works as a shunt active power filter. This mitigates the reactive power, unbalance and harmonic current components of the non-linear loads connected to the PCC during periods of non-peak PV power, all under distorted and unbalanced grid voltage.

2. A dead-beat-based model predictive current control is proposed, developed and validated. At the same time, the proposed current control is aimed to be designed as modular and extensible as possible in order to perform properly, regardless of the bus to which the PC is connected.

The paper is organized as follows. The topology, its operation principle and control scheme are explained in section II, section III shows the performance evaluation of the system under different grid conditions. And finally, Section IV provides the conclusion.

2. System Description

The basic cell of the converter (Figure 1(a)) comprises four power switches (denoted as $S_{1,i}$, $S_{2,i}$, $S_{3,i}$ and $S_{4,i}$, with i denoting each basic cell i), one capacitor ($C_{1,i}$), and an inductor ($L_{1,i}$). This buck-boost converter serves as the fundamental unit or cell for configuring the modular dual-purpose PCs. These PCs act as interfaces between different DERs as PV, ESS or EV, and different ac or dc buses (point of common coupling). A second-order LC filter ($C_{f,i}$ and $L_{f,i}$) with passive damping ($R_{f,i}$) has been selected to mitigate the propagation of higher harmonic components.

This basic buck-boost cell operates in a unipolar mode. As stated above, each cell generates a dc-biased sinusoidal PWM voltage waveform, with a sinusoidal component phase-shifted 2π/3 radians relative to the other. One way to connect a DER to a three-phase four-wire grid is by means of four basic buck-boost cells. This system is schematized in Figure 1(b). Dc to dc power conversion involves parallelizing these n cells and implementing interleaved operation [12].

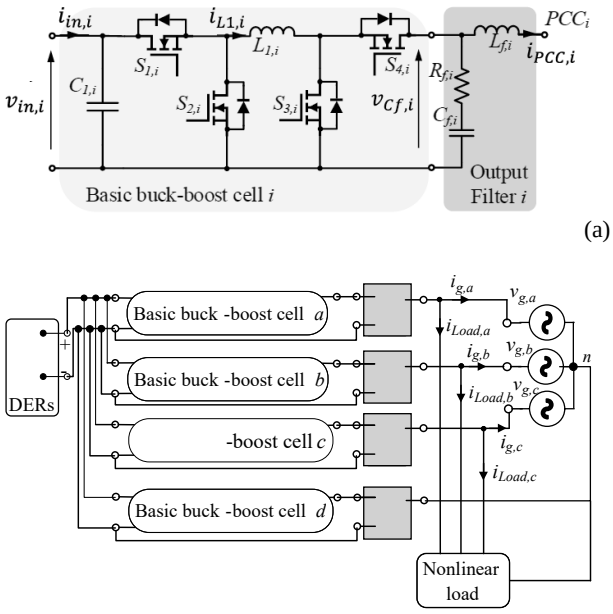

Figure 1. (a) Basic cell of the dual-purpose dc-dc/ac modular power converter. (b) Four cells for dc-ac conversion.

According to the dual-purpose and modularity features required, four scenarios are considered in previous works, i.e: i) from dc to three-phase three-wire ac bus. ii) from dc to a three-phase four-wire ac bus. iii) from dc to unipolar dc bus and iv) from dc to a bipolar dc bus. The present paper is focussed on the interaction of PV panels with a four-wire LV grid (which is typical in Europe), therefore, only scenario ii) will be considered; and this is precisely the case shown in Figure 1(b).

A. Reference current generation

Figure 2 shows the block diagram of the inverter control system. Vector $\mathbf{v_g} = \left(v_{g\,a}\ v_{g\,b}\ v_{g\,c}\right)^T$ represents phase-to-neutral grid voltages. The reference inverter output currents $\mathbf{i^*_{PCC}} = (i^*_{PCC\,a}\ i^*_{PCC\,b}\ i^*_{PCC\,c})^T$ are calculated aiming that either (a) the maximum power is extracted from the PV panels, measuring PV voltage $v_{in} = V_{PV}$ and PV current $i_{in} = I_{PV}$, (this is the MPPT mode, using the classical perturb and observe algorithm), or that (b) the active power P^* setpoint is fulfilled (this is the RPP mode).

In addition, the inverter could be assigned a three-phase fundamental reactive power setpoint ($Q_1^* > 0$ to be injected or $Q_1^* < 0$ to be absorbed), for reasons such as reactive power management in the installation or to provide voltage support at the PCC.

The reference currents, expressing the three-phase quantities in the power invariant synchronous reference frame 0dq (Park transformation), $\mathbf{i}^*_{PR(0dq)}$ and $\mathbf{i}^*_{Q(0dq)}$, are calculated from the set points P^* and Q_1^*, respectively, using the expressions shown in the corresponding blocks of the Figure 2.

Besides, if the inverter rated current I_N is not exceeded, harmonics and unbalanced currents demanded by the nonlinear load $\mathbf{i^*_{Load}} = (i^*_{Load\,a}\ i^*_{Load\,b}\ i^*_{Load\,c})^T$ are completely or partially compensated at the PCC. For this purpose, a strategy is used aiming that the inverter supply the harmonic and fundamental unbalanced components of $\mathbf{i}_{Load}$, that is:

$$\mathbf{i}_{HI}^{*} = \mathbf{i}_{Load} - \mathbf{i}_{Load\,1}^{+}. \quad (1)$$

The synchronous reference frame (SRF) block is in charge to extract $\mathbf{i}_{Load\,1}^{+}$ from the load current vector $\mathbf{i}_{Load}$, by using the positive-sequence fundamental phase angle provided by the ASRF block; thus obtaining the angle of $\mathbf{i}_{Load\,1}^{+}$ with respect to the angle of $\mathbf{u}_1^{+}$.

The reference current in (5) must be saturated to ensure the inverter does not exceed its nominal current I_N. Therefore, the maximum RMS value of the reference current for the *HI* mode is obtained as

$$I_{HI,\max} = \sqrt{I_N^2 - I_P^2 - I_Q^2}\,, \quad (2)$$

where I_P and I_Q are the RMS values for $\mathbf{i}_P^{*}$ and $\mathbf{i}_Q^{*}$, respectively. Finally, the reference current vector is obtained from the equations below.

$$\begin{aligned} \mathbf{i}_{HI}^{*} &= \mathbf{i}_{Load} - \mathbf{i}_{Load1}^{+} && \text{if } I_{HI} \le I_{HI,\max} \\ \mathbf{i}_{HI}^{*} &= (\mathbf{i}_{Load} - \mathbf{i}_{Load1}^{+})\,\frac{I_{HI,\max}}{I_{HI}} && \text{if } I_{HI} > I_{HI,\max} \end{aligned}, \quad (3)$$

where I_{HI} is the highest RMS value of the components of $\mathbf{i}_{HI}^{*}$. This task is carried out by block "saturation".

Although applied to a different power topology, the calculation of this reference currents follows the guidelines detailed in [13], based on the instantaneous power theory, using the power-invariant Park transformation, expressing the three-phase magnitudes in the synchronous reference frame 0*dq*.

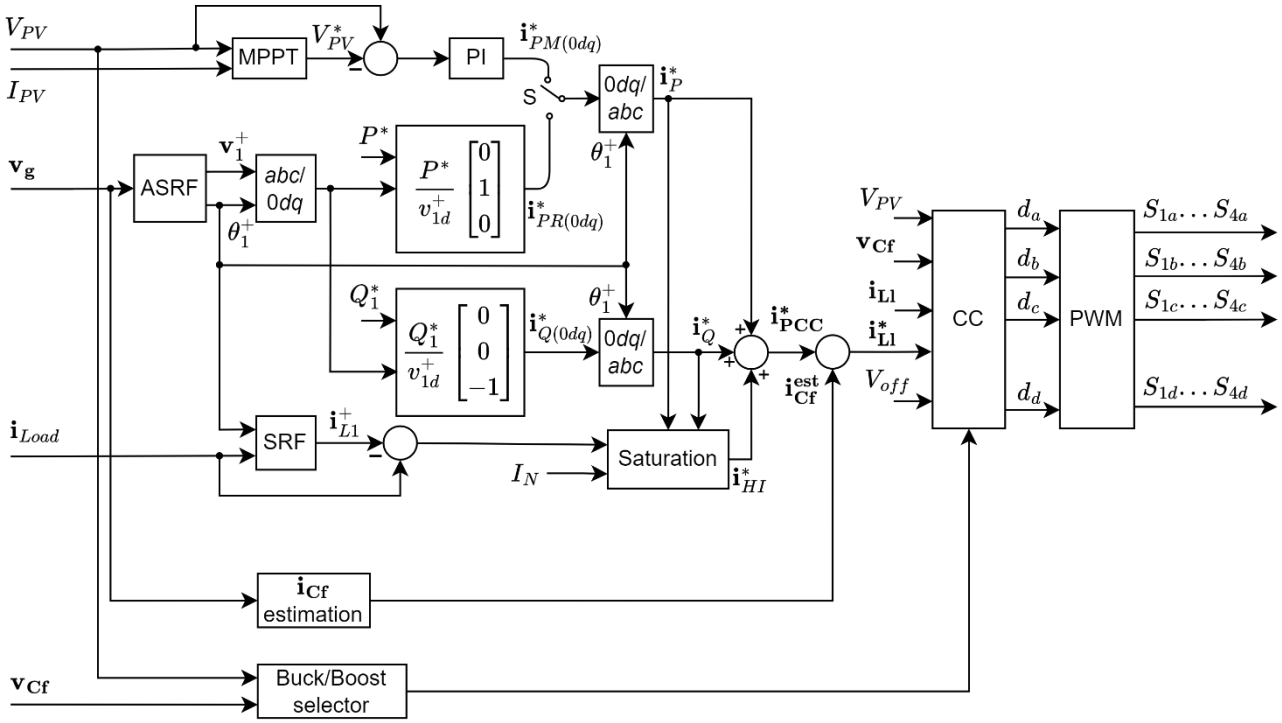

Figure 2. Block diagram of the inverter control system.

B. Current Controller

Once the reference currents have been calculated, the current controller (the block labelled 'CC' in Figure 2) ensures that the inverter's output currents follow these references. A deadbeat control technique is used for this purpose. This is a well-known discrete control technique based on the idea of reducing to zero the error in the controlled variable at the end of the control period. The operation principle applied in this paper is developed in the reference [14]. According to that work, the control law to track any desired reference current $i_{L1,i}^{*}$ are given as follows:

- If $v_{in} > v_{Cf,i}$ during the power conversion of the basic buck-boost cell, then the cell operates in buck mode with $S_{1,i}$ and $S_{2,i}$ switching, and $S_{3,i}$ and $S_{4,i}$ are OFF and ON respectively, and the duty cycle to be applied by $S_{1,i}$ (denoted as $D_{S1,i}$) is

$$D_{S1,i} = \frac{L_{1,i}(i_{L1,i}^{*}(t) - i_{L1,i}(t))}{T_S v_{in}} + \frac{v_{Cf,i}}{v_{in}} \quad (4)$$

- If $v_{in} < v_{Cf,i}$ during the PC operation, then the basic cell operates in boost mode with $S_{1,i}$ and $S_{2,i}$ in ON and OFF states respectively, meanwhile $S_{3,i}$ and $S_{4,i}$ are switching at high frequency. And the duty cycle to be applied by $S_{3,I}$ is

$$D_{S3,i} = \frac{L_{1,i}(i_{L1,i}^{*}(t) - i_{L1,i}(t))}{T_S v_{Cf,i}} - \frac{v_{in}}{v_{Cf,i}} + 1 \quad (5)$$

As one can see, the reference current that appears in the previous equations ($i_{L1,i}^{*}$) must be related to the reference current at the PCC (i^{*}_{PCCi}), which is determined by the reference current generator. Observing Fig. 1(a), and taking into account the states of power switches $S_{1,i}$, $S_{2,i}$, $S_{3,I}$, $S_{4,i}$, in buck and boost modes, respectively, the following relations are derived.

- For buck mode:

$$i^*_{L1,i\ BUCK} = i^*_{PCC,i} + i^{\text{est}}_{Cf,i} \quad (6)$$

- For boost mode:

$$i^*_{L1,i\ BUCK} = (i^*_{PCC,i} + i^{\text{est}}_{Cf,i})\frac{v_{Cf,i}}{v_{in}} \quad (7)$$

The current through the output filter capacitor $\mathbf{i^{est}_{Cf}} = \left(i^{\text{est}}_{Cf\ a}\ i^{\text{est}}_{Cf\ b}\ i^{\text{est}}_{Cf\ c}\right)^T$ can be estimated from the steady state relation, which is represented by its transfer function:

$$i^{\text{est}}_{Cf,i} = \frac{v_{g,i}C_{f,i}s}{R_dC_{f,i}s+1} \quad (8)$$

Operation in buck or boost mode is changed by comparator included in the "Buck/Boost selector" block.

In this case of supplying a three-phase four-wire system, the fourth branch, acting as source neutral-wire, has to synthesize a dc voltage equal to V_{off}. This value is also an input for the "CC" block.

Finally, the modulating signals d_a, d_b; d_c, d_d are the inputs for the PWM block, which is responsible for generating the switching signals for the power electronics $S_{1,i}$, $S_{2,i}$, $S_{3,i}$ and $S_{4,i}$ for each module.

3. Simulation Results

A simulation model for the inverter has been developed in the simulation tool PLECS (from Plexim GmbH).

The dc source consists of a set of commercial photovoltaic panels (3 strings in parallel, 20 panels per string), which together have the following electrical characteristics:

- Maximum power: 3900 W.
- Maximum power point voltage: 352 V.
- Maximum power point current: 11.07 A.
- Short-circuit current: 11.97 A.
- Open-circuit voltage: 434 V.

A 230/400 V 50 Hz three-phase four-wire LV network is considered, which is assumed to be distorted and unbalanced according to the limits indicated in [15], [16]. Individual distortion percentage for third harmonic is selected at its limit (5%), while for fifth and seventh harmonics the percentages (4.5% and 4%, respectively) are calculated for having a total harmonic distortion (THD) below the 8% limit. The inverse- and zero- to positive-sequence component ratios are set over the limits ($V^-/V^+ = V^0/V^+ = 3.77$ %).

The effectiveness of an APF is assessed by incorporating an unbalanced and non-linear load. As stated in [17], harmonic analysis and corrective actions are necessary in commercial buildings and industrial facilities when a significant portion of the load (usually exceeding 25% to 30%) consists of non-linear loads or is expected to include them. In this work, as a demanding situation, a non-linear load connected at the PCC is considered, which demands a current whose positive sequence fundamental component is set at 30 % of the rated current of the equipment, and whose unbalance and odd harmonic content up to the 9th order is specified in Table I, according to IEC TS 61000-3-4 [18]. Figure 3 shows the waveform of both, the phase-to-neutral grid voltages and the load currents.

Key parameters of the power electronic converter, taking into account the characteristics of the aforementioned PV panels and LV grid, calculated according to [2] and [14], are listed in Table II.

TABLE I. HARMONIC CONTENT OF THE NON-LINEAR LOAD.

Individual Harmonic Distortion (% Respect to the Positive-Sequence Fundamental Component)				Total Harmonic Distortion THD (%)	I^-/I^+ (%)	I^0/I^+ (%)
HD3	HD5	HD7	HD9			
21.6	10.7	7.2	3.8	25.44	10	10

I^+, I^-, I^0: positive-, negative- and zero-sequence fundamental components.

TABLE II. MAIN PARAMETERS AND VALUES

	Parameter	Value
	Rated power	4000 W
	Input voltage (v_{in})	340 – 450 V
	Voltage bias (V_{off})	400 V
Basic cell	Switching frequency (f_s)	50 kHz
	Input capacitor ($C_{1,i}$)	500 µF
	Cell inductor ($L_{1,i}$)	1.6 mH
	Cell resistance inductor	0.1 Ω
Filter	Filter capacitor ($C_{f,i}$)	4.7 µF
	Damping resistor ($R_{f,i}$)	3 Ω
	Filter inductor ($L_{f,i}$)	1.273 mH
	Filter resistance inductor	0.1 Ω

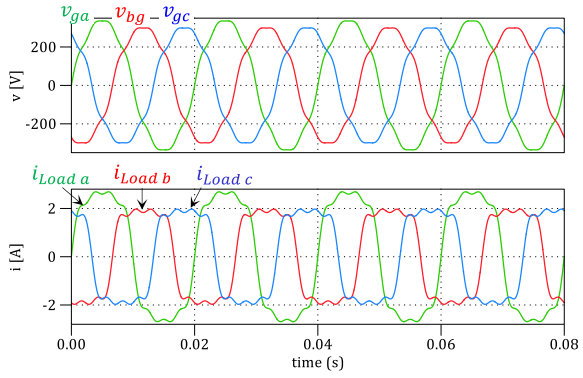

Figure 3. Top: Phase-to-neutral grid voltages distorted and unbalanced according to the limits indicated in [14] and [15]. Bottom: Unbalanced and non-linear load currents.

From the full simulation span, the most representative cases and signals were selected. Figure 4 demonstrates the correctness of the APF functionality. For this case the operation conditions are: PV panels in STC (Standard Test Condition, irradiance 1000 W/m^2, temperature 25ºC), converter in MPPT mode, $Q_1^* = 0$, HI mode is activated at t = 0.24 s. Before HI activation, despite the unbalanced and distorted grid voltages, the inverter output currents waveforms are balanced and sinusoidal. However, since load current is unbalanced and distorted, the currents

injected into the grid are unbalanced and distorted. After HI function, consequently, inverter currents become distorted and unbalanced so that the grid currents tend to be balanced and sinusoidal. Figure 5 illustrates the behaviour in case of a step change of the reactive power setpoint, and the saturation or compensation limit. The conditions are the same as for the previous figure. At t = 0.34 s, the setpoint for Q_1 is adjusted to $Q_1^* = 2000$ VAr. Under these conditions, the compensation requirements cannot be met without causing equipment overload. Consequently, the inverter provides partial compensation, resulting in grid currents that are neither sinusoidal nor balanced anymore.

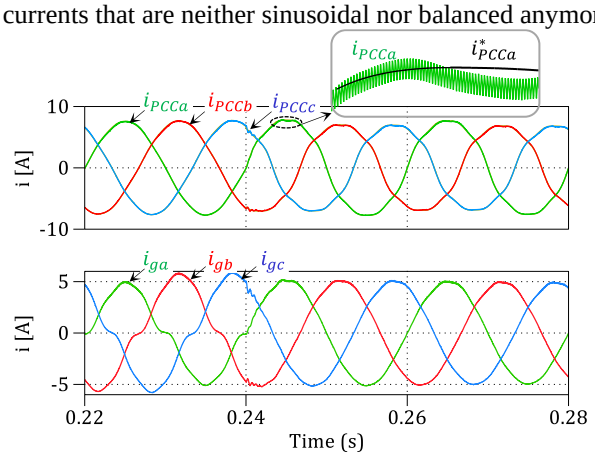

Figure 4. Simulation results. APF function. At t = 0.24 s, HI function is activated. Top: inverter output currents ($i_{PCC\,a}$, $i_{PCC\,b}$, $i_{PCC\,c}$) and references ($i^*_{PCC\,a}$, $i^*_{PCC\,b}$, $i^*_{PCC\,c}$). Bottom: grid currents (i_{ga} , i_{gb} , i_{gc}).

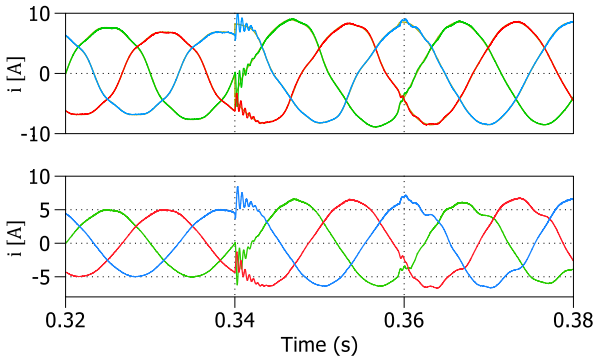

Figure 5. Simulation results. Setpoint changes. Initially is Q_1^* = 0; at t = 0.34 s, reactive power setpoint change to 2000 VAr. Top: inverter output currents ($i_{PCC\,a}$, $i_{PCC\,b}$, $i_{PCC\,c}$) and references ($i^*_{PCC\,a}$, $i^*_{PCC\,b}$, $i^*_{PCC\,c}$). Bottom: grid currents (i_{ga} , i_{gb} , i_{gc}).

4. Conclusion

In this work, dc–dc and dc–ac three-phase universal converter, based on dc-dc buck-boost cell topology is applied as PV inverter, controlling the active power injected into the grid (extracting the maximum or a reference power from PV panels) and operating as a shunt active power filter simultaneously. An improved deadbeat current controller was programmed and successfully tested.

The performance of the inverter has been investigated extensively. Simulation study tests have proven a proper operation as an APF, under unbalanced and distorted grid voltages, in the presence of a very demanding case of unbalanced and non-linear load, for different PV voltages and different active and reactive power setpoints.

Given that the proposed system's features are especially well-suited for high-power applications, such as those in commercial and industrial settings or multi-megawatt PV plants, this paper emphasizes the idea of utilizing the converters in these installations for the provision of ancillary services to the grid.

References

[1] O. Husev, O. Matiushkin, D. Vinnikov, C. Roncero-Clemente, and S. Kouro, “Novel concept of solar converter with universal applicability for DC and AC microgrids,” IEEE Trans. Ind. Electron., vol. 69, no. 5, pp. 4329–4341, May 2022.

[2] C. Roncero-Clemente et al., "Feasibility Study of Three-Phase Modular Converter for Dual-Purpose Application in DC and AC Microgrids," in IEEE Journal of Emerging and Selected Topics in Power Electronics, doi: 10.1109/JESTPE.2023.3247960.

[3] O. Husev, D. Vinnikov, S. Kouro, F. Blaabjerg and C. Roncero-Clemente, "Dual-Purpose Converters for DC or AC Grid as Energy Transition Solution: Perspectives and Challenges," in IEEE Industrial Electronics Magazine, doi: 10.1109/MIE.2022.3230219.

[4] O. Husev, O. Matiushkin, T. Jalakas, D. Vinnikov and N. V. Kurdkandi, "Comparative Evaluation of Dual-Purpose Converters Suitable for Application in dc and ac Grids," in IEEE Journal of Emerging and Selected Topics in Power Electronics, doi: 10.1109/JESTPE.2023.3243857.

[5] M. Antivachis, N. Kleynhans and J. W. Kolar, "Three-Phase Sinusoidal Output Buck-Boost GaN Y-Inverter for Advanced Variable Speed AC Drives," in IEEE Journal of Emerging and Selected Topics in Power Electronics, vol. 10, no. 3, pp. 3459-3476, June 2022, doi: 10.1109/JESTPE.2020.3026742.

[6] A. Y. Farag, D. Biadene, P. Mattavelli and T. Younis, "Three-Phase Four-Wire Step-Down Modular Converter for an Enhanced Interlinking in Low-Voltage Hybrid AC/DC Microgrids," in IEEE Open Journal of Power Electronics, vol. 5, pp. 634-647, 2024, doi: 10.1109/OJPEL.2024.3394548.

[7] K. P. Gokhale, A. Kawamura, and R. G. Hoft, Dead beat microprocessor control of PWM inverter for sinusoidal output waveform synthesis, IEEE Trans. Ind. Appl., vol. IA-23, no. 5, pp. 901910, Sep. 1987.

[8] A. Zama, A. Benchaib, S. Bacha, D. Frey, S. Silvant, and D. Georges, Linear feedback dead-beat control for modular multilevel converters: Validation under faults grid operation mode, IEEE Trans. Ind. Electron., vol. 68, no. 4, pp. 3181 3191, Apr. 2021.

[9] J.-H. Lee and K.-B. Lee, A dead-beat control for bridgeless inverter systems to reduce the distortion of grid current, IEEEJ.Emerg.Sel.Topics Power Electron., vol. 6, no. 1, pp. 151164, Mar. 2018.

[10] S.Buso,T. Caldognetto, and D. Iglesias Brandao, Dead-beat current controller for voltage-source converters with improved large-signal response, IEEE Trans. Ind. Appl., vol. 52, no. 2, pp. 15881596, Apr. 2016.

[11] N. Gao, Z. Jin, H. Wang, W. Wu, E. Koutroulis, H. S.-H. Chung, and F. Blaabjerg, MOSFET-switch-based transformerless single-phase gridtied inverter for PV systems, IEEE J. Emerg. Sel. Topics Power Electron., early access, Mar. 9, 2021, doi: 10.1109/JESTPE.2021.3064587.

[12] G. J. Capella, J. Pou, S. Ceballos, G. Konstantinou, J. Zaragoza and V. G. Agelidis, "Enhanced Phase-Shifted PWM Carrier Disposition for Interleaved Voltage-Source Inverters," in IEEE Transactions on Power Electronics, vol. 30, no. 3, pp. 1121-1125, March 2015, doi: 10.1109/TPEL.2014.2338357.

[13] F. Barrero-González, C. Roncero-Clemente, J. Gutiérrez-Escalona, M. I. Milanés-Montero, E. González-Romera and E. Romero-Cadaval, "Three-Level T-Type Quasi-Z Source PV Grid-Tied Inverter with Active Power Filter Functionality Under Distorted Grid Voltage," in IEEE Access, vol. 10, pp. 44503-44516, 2022, doi: 10.1109/ACCESS.2022.3170098.

[14] C. Roncero-Clemente, J. -G. Escalona, V. F. Pires, O. Matiushkin, M. I. Milanés-Montero and E. Romero-Cadaval, "Dead-Beat-based Model Predictive Current Control for the Dual-Purpose dc-dc/ac PWM Modular Power Converter," 2024 IEEE 18th International Conference on Compatibility, Power Electronics and Power Engineering (CPE-POWERENG), Gdynia, Poland, 2024, pp. 1-6, doi: 10.1109 /CPE-POWERENG60842.2024.10604328.

[15] Voltage Characteristics of Electricity Supplied by Public Electricity Networks, Standard EN 50160:2010; CENELEC, Brussels, Belgium, 2015.

[16] Electromagnetic Compatibility (EMC) Part 22: Environment Compatibility Levels for Low-Frequency Conducted Disturbances and Signalling in Public Low-Voltage Power Supply Systems, Standard IEC 61000-2-2, International Electrotechnical Commission: Geneva, Switzerland, 2002.

[17] IEEE Recommended Practice for Conducting Harmonic Studies and Analysis of Industrial and Commercial Power Systems, IEEE Standard 3002.8-2018, Piscataway, NJ, USA, 2018, pp. 1-79.

[18] Electromagnetic compatibility (EMC)-Part 3-4: Limits-Limitation of emission of harmonic currents in low-voltage power supply systems for equipment with rated current greater than 16 A. In IEC TS 61000-3-4:1998; International Electrotechnical Commission, Genève, Switzerland, 1998.